Science
AAAS

A Gene Network Regulating Lysosomal Biogenesis and Function

Marco Sardiello, *et al.*

Science **325**, 473 (2009);
DOI: 10.1126/science.1174447

Science (print ISSN 0036-8075; online ISSN 1095-9203) is published weekly, except the last week in December, by the American Association for the Advancement of Science, 1200 New York Avenue NW, Washington, DC 20005.

activation in the presumptive neurogenic ectoderm (*29*), identified by ChIP-chip assays for the DV regulatory genes Dorsal, Twist, and Snail (*30*). Shadow enhancers might compensate for fluctuations in Dorsal concentrations by increasing the probability of occupancy of critical Dorsal binding sites (*10*, *29*–*33*). In contrast, neither of the genes that display stochastic activation in *dl*/+ embryos (*rho* and Neu3) appear to contain shadow enhancers (Fig. 4C). However, these results are preliminary, and definitive evidence that shadow enhancers provide an adaptive response to genetic perturbations will require additional study.

Previous visualization studies failed to distinguish synchronous and stochastic modes of gene activation (*12*–*18*, *20*, *21*, *23*, *27*, *30*, *34*–*36*). This finding was made possible by the use of a quantitative method that examines gene expression in many embryos rather than just a few individual embryos. Most DV patterning genes contain stalled Pol II (*37*), and we predict that most of these genes exhibit synchronous patterns of induction.

Pol II stalling and transcriptional synchrony may help to ensure the orderly unfolding of the complex genetic programs that control development. It is likely that any given gene, or even small sets of genes, can be activated in a stochastic fashion without causing severe patterning defects. However, the reproducible and reliable development of large populations of embryos might be incrementally augmented by the acquisition of stalled Pol II on critical developmental control genes.

References and Notes

1. A. Raj, C. S. Peskin, D. Tranchina, D. Y. Vargas, S. Tyagi, *PLoS Biol.* **4**, e309 (2006).
2. A. Raj, A. van Oudenaarden, *Cell* **135**, 216 (2008).
3. J. M. Raser, E. K. O'Shea, *Science* **304**, 1811 (2004); published online 27 May 2004 (10.1126/science.1098641).
4. J. M. Raser, E. K. O'Shea, *Science* **309**, 2010 (2005).
5. D. A. Hendrix, J. W. Hong, J. Zeitlinger, D. S. Rokhsar, M. S. Levine, *Proc. Natl. Acad. Sci. U.S.A.* **105**, 7762 (2008).
6. J. T. Lis, *Nature* **450**, 198 (2007).
7. S. Bergmann *et al.*, *PLoS Biol.* **5**, e46 (2007).
8. M. Coppey, A. N. Boettiger, A. M. Berezhkovskii, S. Y. Shvartsman, *Curr. Biol.* **18**, 915 (2008).
9. T. Gregor, W. Bialek, R. R. d. R. van Steveninck, D. W. Tank, E. F. Wieschaus, *Proc. Natl. Acad. Sci. U.S.A.* **102**, 18403 (2005).
10. T. Gregor, D. W. Tank, E. F. Wieschaus, W. Bialek, *Cell* **130**, 153 (2007).
11. T. Gregor, E. F. Wieschaus, A. P. McGregor, W. Bialek, D. W. Tank, *Cell* **130**, 141 (2007).
12. A. Stathopoulos, M. Van Drenth, A. Erives, M. Markstein, M. Levine, *Cell* **111**, 687 (2002).
13. S. N. Maity, B. de Crombrugghe, *Trends Biochem. Sci.* **23**, 174 (1998).
14. M. K. Baylies, A. M. Michelson, *Curr. Opin. Genet. Dev.* **11**, 431 (2001).
15. A. M. Michelson, S. Gisselbrecht, E. Buff, J. B. Skeath, *Development* **125**, 4379 (1998).
16. M. Y. Zhu, R. Wilson, M. Leptin, *Genetics* **170**, 767 (2005).
17. F. Imam, D. Sutherland, W. Huang, M. A. Krasnow, *Genetics* **152**, 307 (1999).
18. M. Leptin, M. Affolter, *Curr. Biol.* **14**, R480 (2004).
19. S. Ricardo, R. Lehmann, *Science* **323**, 943 (2009).
20. T. Gryzik, H. A. Muller, *Curr. Biol.* **14**, 659 (2004).
21. A. Stathopoulos, B. Tam, M. Ronshaugen, M. Frasch, M. Levine, *Genes Dev.* **18**, 687 (2004).
22. P. Ramain, P. Heitzler, M. Haenlin, P. Simpson, *Development* **119**, 1277 (1993).
23. L. H. Frank, C. Ruschlow, *Development* **122**, 1343 (1996).
24. A. M. Huang, J. Rusch, M. Levine, *Genes Dev.* **11**, 1963 (1997).
25. P. M. Macdonald, G. Struhl, *Nature* **336**, 595 (1988).
26. Y. T. Ip, R. E. Park, D. Kosman, K. Yazdanbakhsh, M. Levine, *Genes Dev.* **6**, 1518 (1992).
27. R. P. Zinzen, K. Senger, M. Levine, D. Papatsenko, *Curr. Biol.* **16**, 1358 (2006).
28. S. Gonzalez-Crespo, M. Levine, *Genes Dev.* **7**, 1703 (1993).
29. J.-W. Hong, D. A. Hendrix, M. S. Levine, *Science* **321**, 1314 (2008).
30. J. Zeitlinger *et al.*, *Genes Dev.* **21**, 385 (2007).
31. H. C. Berg, E. M. Purcell, *Biophys. J.* **20**, 193 (1977).
32. W. Bialek, S. Setayeshgar, *Phys. Rev. Lett.* **100**, 258101 (2008).
33. G. Tkacik, T. Gregor, W. Bialek, *PLoS One* **3**, e2774 (2008).
34. E. Bier, L. Y. Jan, Y. N. Jan, *Genes Dev.* **4**, 190 (1990).
35. V. Francois, M. Solloway, J. W. O'Neill, J. Emery, E. Bier, *Genes Dev.* **8**, 2602 (1994).
36. J. B. Skeath, G. F. Panganiban, S. B. Carroll, *Development* **120**, 1517 (1994).
37. J. Zeitlinger *et al.*, *Nat. Genet.* **39**, 1512 (2007).

38. We thank P. Ralph and S. Evans for help with constructing and analyzing the mathematical models of Pol II elongation and initiation that motivated our hypothesis about the synchrony of gene expression. A.N.B. is supported by NSF Graduate Research Fellowship Program. This study was funded by a grant from NIH (GM34431).

Supporting Online Material

www.sciencemag.org/cgi/content/full/325/5939/471/DC1
SOM Text
Figs. S1 to S7
Table S1
References

24 March 2009; accepted 4 June 2009
10.1126/science.1173976

A Gene Network Regulating Lysosomal Biogenesis and Function

Marco Sardiello,[1] Michela Palmieri,[1] Alberto di Ronza,[1] Diego Luis Medina,[1] Marta Valenza,[2] Vincenzo Alessandro Gennarino,[1] Chiara Di Malta,[1] Francesca Donaudy,[1] Valerio Embrione,[1] Roman S. Polishchuk,[3] Sandro Banfi,[1] Giancarlo Parenti,[1,4] Elena Cattaneo,[2] Andrea Ballabio[1,4]*

Lysosomes are organelles central to degradation and recycling processes in animal cells. Whether lysosomal activity is coordinated to respond to cellular needs remains unclear. We found that most lysosomal genes exhibit coordinated transcriptional behavior and are regulated by the transcription factor EB (TFEB). Under aberrant lysosomal storage conditions, TFEB translocated from the cytoplasm to the nucleus, resulting in the activation of its target genes. TFEB overexpression in cultured cells induced lysosomal biogenesis and increased the degradation of complex molecules, such as glycosaminoglycans and the pathogenic protein that causes Huntington's disease. Thus, a genetic program controls lysosomal biogenesis and function, providing a potential therapeutic target to enhance cellular clearing in lysosomal storage disorders and neurodegenerative diseases.

Lysosomes are specialized to degrade macromolecules received from the secretory, endocytic, autophagic, and phagocytic pathways (*1*). Because degradation requirements of the cell may vary depending on tissue type, age, and environmental conditions, we postulated the presence of a cellular program coordinating lysosomal activity. By using the g:profiler (*2*) tool, we observed that genes encoding lysosomal proteins, hereafter referred to as lysosomal genes, tend to have coordinated expression (figs. S1 and S2). Pattern discovery analysis of the promoter regions of the 96 known lysosomal genes (*3*) resulted in the identification of a palindromic 10–base pair (bp) GTCACGTGAC motif highly enriched in this promoter set (68 genes out of 96; $P < 0.0001$) (fig. S3). This motif is preferentially located within 200 bp from the transcription start site (TSS), either as a single sequence or as tandem multiple copies (fig. S4 and table S1). The distribution of this motif was determined around all human gene TSSs (Fig. 1A), and gene ontology analysis of the genes with at least two motifs within 200 bp from the TSS—suggesting that they are probably in a promoter—showed a significant enrichment for functional categories related to lysosomal biogenesis and function (table S2). Thus, we named this motif Coordinated Lysosomal Expression and Regulation (CLEAR) element. A luciferase assay showed that the CLEAR element mediates transcriptional activation (Fig. 1B).

The CLEAR consensus sequence overlaps that of the E-box (CANNTG), a known target site for basic helix-loop-helix (bHLH) transcription factors (*4*). In particular, members of the microphthalmia–transcription factor E (MiT/TFE) subfamily of bHLH factors were found to bind sequences similar to the CLEAR consensus (*5*). The MiT/TFE subfamily is composed of four members in humans: MITF, TFE3, TFEB, and TFEC (*6*). To determine whether any of these proteins are able to modulate the expression of lysosomal genes, we transfected HeLa cells with plasmids carrying *MITF*, *TFE3*, *TFEB*, or *TFEC*

[1]Telethon Institute of Genetics and Medicine, Via P. Castellino 111, 80131 Naples, Italy. [2]Department of Pharmacological Sciences and Center for Stem Cell Research, University of Milan, Via Balzaretti 9, 20133 Milan, Italy. [3]Telethon Electron Microscopy Core Facility, Department of Cell Biology and Oncology, Consorzio Mario Negri Sud, I-66030 Santa Maria Imbaro, Chieti, Italy. [4]Department of Pediatrics, Federico II University, Via S. Pansini 5, 80131 Naples, Italy.

*To whom correspondence should be addressed. E-mail: ballabio@tigem.it

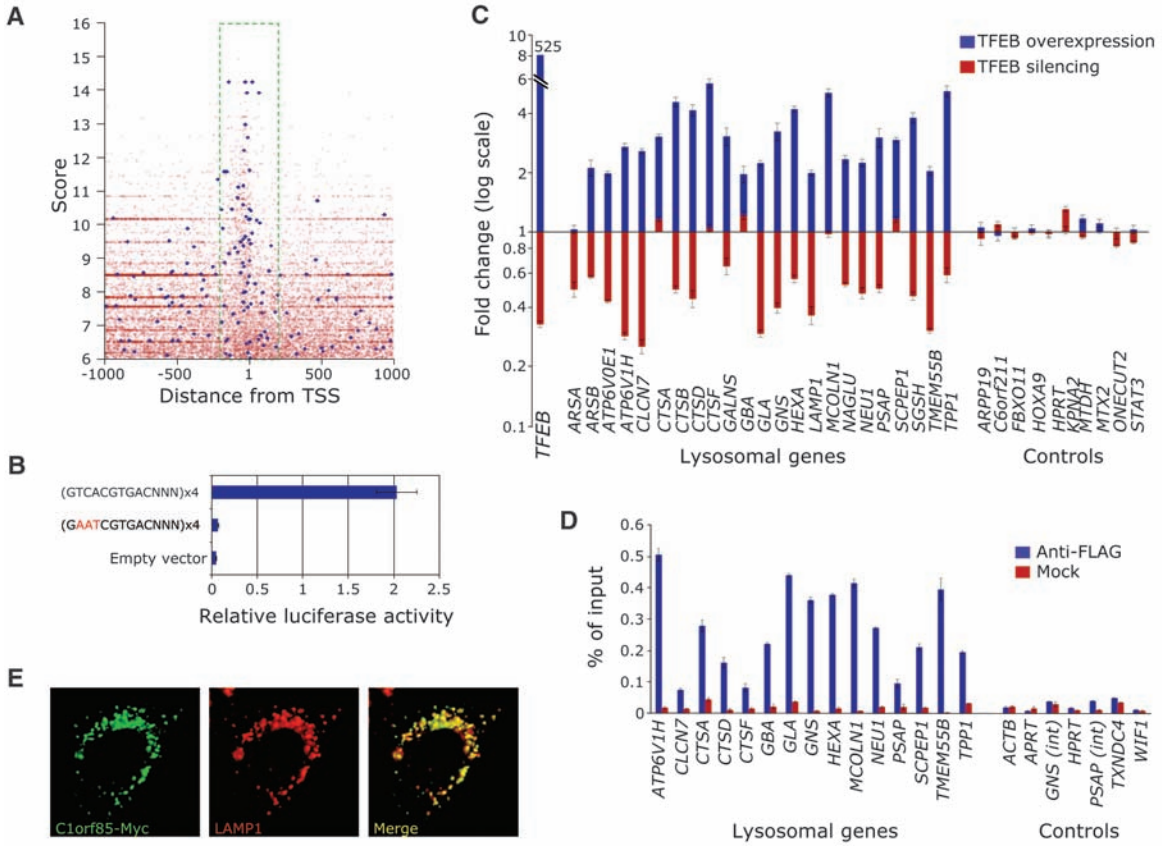

Fig. 1. A regulatory gene network controlling the expression of lysosomal genes. (**A**) Genomic distribution of CLEAR elements (red dots) at human gene promoters. Scores are assigned based on the CLEAR position weight matrix. Blue dots indicate CLEAR elements in the promoters of lysosomal genes. The dashed box contains all the elements corresponding to the genes that were used for Gene Ontology analysis. (**B**) Luciferase assay using constructs carrying four tandem copies of either intact (top) or mutated (middle; mutations in red) CLEAR elements. (**C**) Expression analysis of lysosomal genes after TFEB overexpression and silencing. Blue bars show the fold change of the mRNA levels of lysosomal genes in TFEB- versus pcDNA3-transfected cells. Red bars show the fold change of mRNA levels in mimic-miR-128–transfected cells versus cells transfected with a standard control miRNA (mimic-miR-cel-67). Randomly chosen nonlysosomal genes were used as controls. Gene expression was normalized relative to *glyceraldehyde-3-phosphate dehydrogenase* (*GAPDH*). (**D**) ChIP analysis. The histogram shows the amount of the immunoprecipitated DNA expressed as a percentage of the total input DNA. Controls include promoters of housekeeping genes (*ACTB*, *APRT*, and *HPRT*), random genes lacking CLEAR sites (*TXNDC4* and *WIF1*), and intronic sequences (int) of lysosomal genes. Lysosomal genes and controls were significantly different: Mann-Whitney-Wilcoxon test ($P < 10^{-4}$). All experiments in (B), (C), and (D) were performed in triplicates (data represent mean ± SD). (**E**) Confocal microscopy showing colocalization of C1orf85-Myc (green) with the lysosomal membrane marker LAMP1 (red) in HeLa cells.

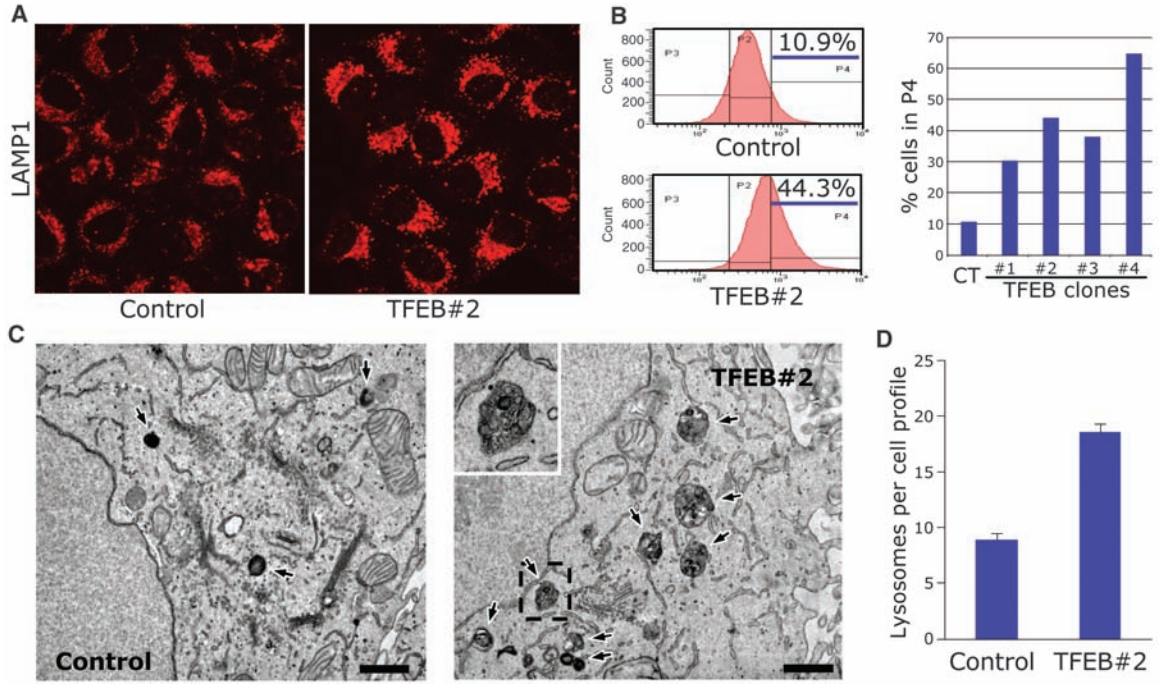

Fig. 2. TFEB overexpression induces lysosomal biogenesis. Comparison of HeLa stable transfectants of either *TFEB* or empty pcDNA3 vector (control). (**A**) Confocal microscopy after staining with an antibody against the lysosomal marker LAMP1. (**B**) Fluorescence-activated cell sorting (FACS) analysis after staining with lysosome-specific dye Lysotracker. The analysis was performed on four independent clones (TFEB#1 to -4) (fig. S12). Blue bars indicate the proportion of cells with fluorescence intensity greater than the indicated threshold (P4 gate). 30,000 cells per clone were analyzed. (**C**) Electron microscopy analysis. Thin sections exhibit more lysosome profiles (arrows) with typical ultrastructure (inset, details corresponding to dash boxed area) in *TFEB*–overexpressing transfectants over the control. Scale bar, 720 nm. (**D**) Number of lysosomes in thin sections (average ± SE, $n = 20$ cells).

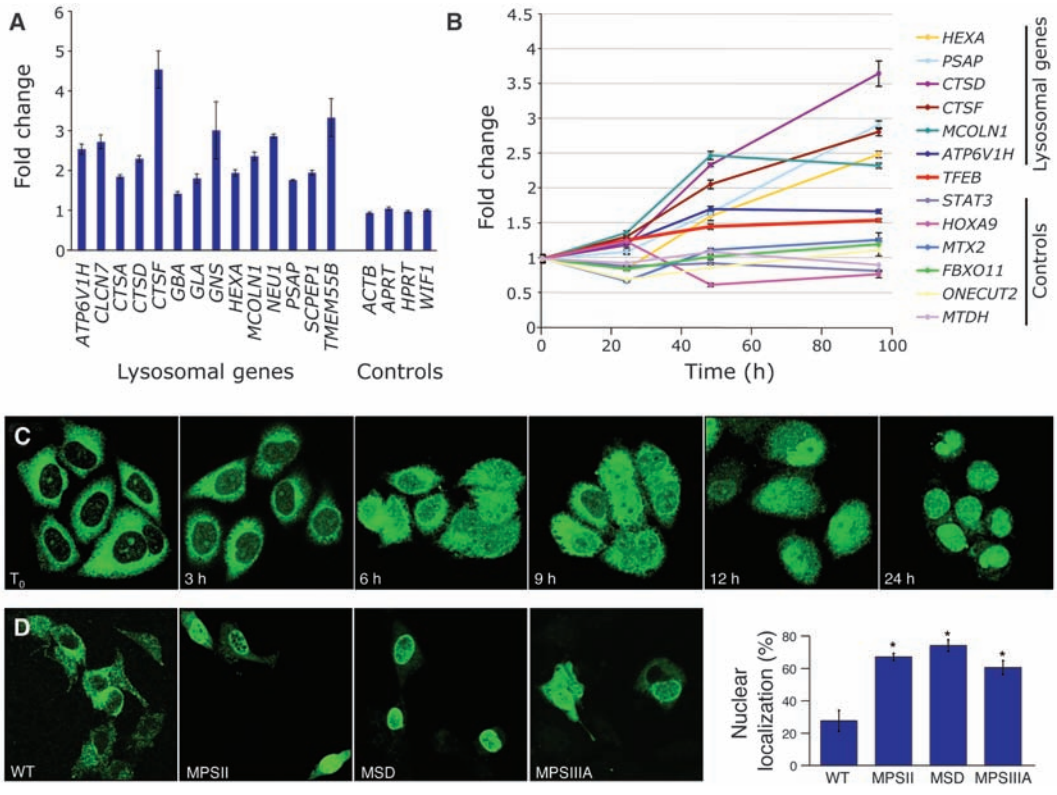

Fig. 3. The CLEAR network is activated by lysosomal storage. (**A**) ChIP analysis following lysosomal storage of sucrose. The histogram shows the ratio (expressed as fold change) between the amounts of FLAG-immunoprecipitated chromatin in sucrose-treated versus non-treated cells. Lysosomal genes show an average two- to three-fold increase of immunoprecipitated chromatin, whereas no significant changes are observed for control genes. (**B**) Expression analysis of lysosomal genes after sucrose supplementation. The diagram shows a time-course analysis of the mRNA levels of lysosomal genes and of *TFEB*. Gene expression was monitored by means of real-time quantitative polymerase chain reaction (PCR) and normalized relative to *GAPDH*. All experiments in (A) and (B) were performed at least in duplicates (data represent mean ± SD). (**C**) Immunofluorescence microscopy analysis of TFEB subcellular localization after sucrose supplementation. HeLa clones stably expressing TFEB-3xFLAG were stained with an antibody to FLAG at various time points after the addition of sucrose in culture medium. (**D**) Immunofluorescence microscopy analysis of TFEB localization in mouse embryonic fibroblasts (MEFs) from mouse models of three different types of LSDs. MEFs from LSD or wild-type (WT) mice were transiently transfected with a TFEB-3xFLAG construct and stained with an antibody to FLAG. The percentages of nuclei positive for FLAG staining were estimated by examining 100 cells per cell type in two different transfection experiments (data represent mean ± SD).

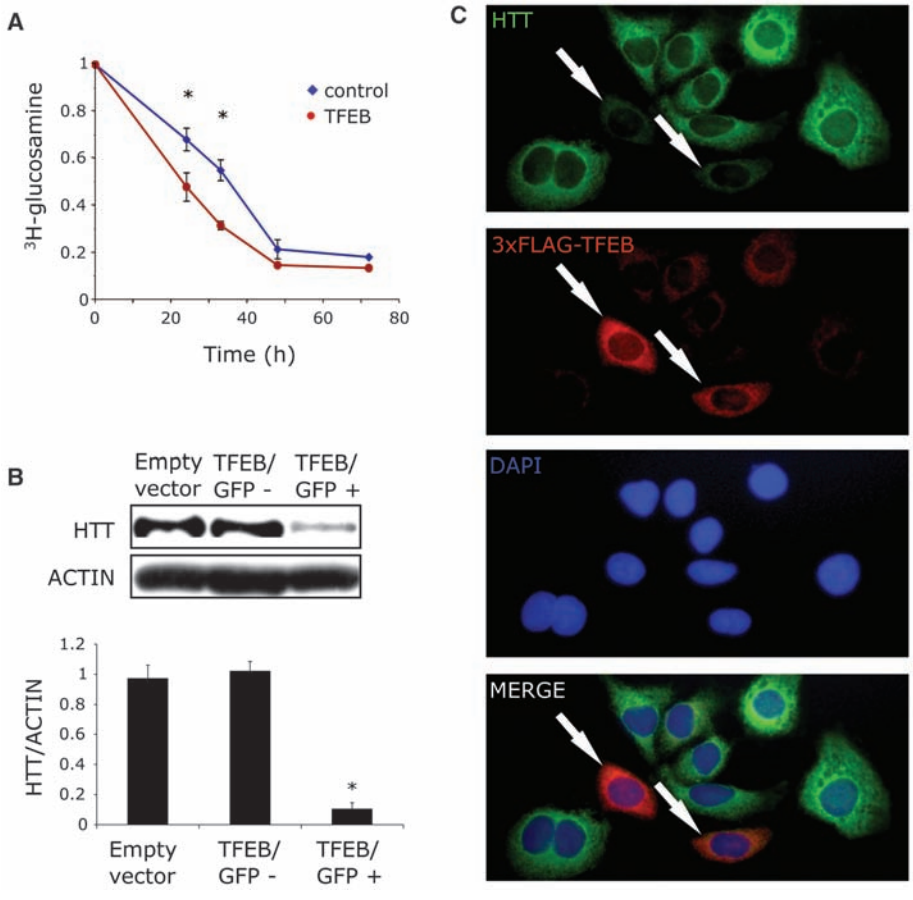

Fig. 4. TFEB enhances cellular clearance. (**A**) Comparison of the kinetics of GAG clearance in HeLa-stable clones of either *TFEB* or empty pcDNA3 vector (control). The graph shows relative amounts of ^{3}H-glucosamine incorporated into GAGs over time. 1 = ^{3}H-glucosamine levels at time zero. *$P < 0.05$. Experiments were performed in triplicates (data represent mean ± SD). (**B** and **C**) Clearance of polyQ-expanded huntingtin (HTT) after TFEB overexpression. (B) Immunoblot analysis of TFEB-EGFP–positive (+) and TFEB-EGFP–negative (–) HD43 cells separated by FACS 24 hours after electroporation. The graph of densitometric analysis shows a strong decrease of polyQ-expanded huntingtin in TFEB-EGFP–positive cells as compared with that in controls. (C) Immunocytochemical analysis of TFEB and HTT in HD43(Q105) cells transfected with 3xFLAG-TFEB construct showing little huntingtin staining in cells positive for 3xFLAG-TFEB staining.

cDNAs. We observed an increase in the mRNA levels of lysosomal genes (22 out of 23 genes tested) only after TFEB overexpression (Fig. 1C). Accordingly, we detected a significant increase in the activities of lysosomal enzymes β-glucosidase, Cathepsin D, and β-glucuronidase (fig. S5). Induction of lysosomal genes after TFEB overexpression was also observed in human embryonic kidney (HEK) 293 cells (fig. S6). We predicted that TFEB could be a target of the microRNA miR-128 (*7*), which was confirmed by luciferase experiments (fig. S7). TFEB silencing mediated by miRNA was associated with the downregulation of 18 out of the 23 lysosomal genes tested (Fig. 1C and fig. S8). Thus, TFEB regulates the expression of lysosomal genes.

To test whether lysosomal genes are direct targets of TFEB, we performed chromatin immunoprecipitation (ChIP) analysis on HeLa cells that stably express a TFEB 3xFLAG construct using an antibody to FLAG. The results demonstrated that TFEB binds to CLEAR sites (Fig. 1D). To identify genes responsive to TFEB on a genomic scale, we performed microarray analysis of the HeLa transcriptome after TFEB overexpression. We observed that 291 genes were upregulated and seven were down-regulated, at a false discovery rate of <0.1 (table S3). Upregulated genes were greatly enriched with lysosomal genes and genes related to lysosomal biogenesis and function (figs. S9 and S10 and table S4). Accordingly, gene set enrichment analysis (GSEA) showed a significant enrichment (enrichment score = 0.84; $P < 0.0001$) of lysosomal genes that contain CLEAR elements in their promoters among induced genes (fig. S11). Nonlysosomal genes involved in degradation pathways appear to be modulated by TFEB. These include *RRAGC* and *UVRAG*, which are key factors regulating autophagy (*8*, *9*); *CSTB*, which plays a role in protecting against the proteases leaking from lysosomes (*10*); and *M6PR* and *IGF2R*, which mediate the import of proteins into the lysosome (*11*). To illustrate the feasibility of using the CLEAR network as a tool to identify genes involved in lysosomal function and to provide candidate genes for orphan lysosomal diseases (*3*), we determined the subcellular distribution of two randomly chosen proteins of unknown function, *C1orf*85 and *C12orf*49. The uncharacterized TFEB target, *C1orf85*, was found localized to lysosomes (Fig. 1E).

An expansion of the lysosomal compartment was detected in HeLa transfectants that stably overexpress TFEB (Fig. 2, A and B, and fig. S12). Accordingly, ultrastructural analysis revealed a significant increase in the number of lysosomes per cell (Fig. 2, C and D), indicating the involvement of TFEB in lysosomal biogenesis. This is similar to MITF, another member of the MiT/TFE family, which is involved in a related cellular function, melanosomal biogenesis (*6*).

An increase of the expression levels of lysosomal genes and of genes involved in cholesterol biosynthesis and intracellular trafficking was previously reported in a sucrose-induced vacuolation model (*12*, *13*). We used this model to test whether the TFEB-CLEAR network responds to lysosomal storage of undegraded molecules. An increase of the binding events of TFEB to lysosomal promoters (Fig. 3A) and of the mRNA levels of lysosomal genes, and to a lesser extent of *TFEB*, was detected upon sucrose supplementation to the culture medium (Fig. 3B). The addition of sucrose also determined the progressive translocation of TFEB from a diffuse localization in the cytoplasm, where it predominantly resides in untreated cells, to the nucleus (Fig. 3C), suggesting that nuclear translocation is an important mechanism for TFEB activation.

Over 40 lysosomal storage disorders (LSDs) are characterized by the progressive accumulation of undigested macromolecules within the cell, resulting in cellular dysfunction that leads to diverse clinical manifestations (*1*, *14*, *15*). We investigated TFEB subcellular localization in embryonic fibroblasts obtained from mouse models of three different LSDs, Mucopolysaccharidoses types II and IIIA (MPSII and MPSIIIA) and Multiple Sulfatase Deficiency (MSD) (*16*–*18*). A predominant nuclear localization of TFEB was detected in cells from all three LSD mouse models (Fig. 3D), suggesting that the TFEB signaling pathway is activated after the intralysosomal storage of undegraded molecules. Such activation could be part of the cellular physiological response to lysosomal stress and could serve degradation needs by enhancing the lysosomal system.

To test the ability of TFEB to enhance lysosome-dependent degradation pathways, we analyzed the degradation of glycosaminoglycans (GAGs) in a pulse-chase experiment. TFEB stable transfectants displayed a faster rate of GAG clearance as compared with that in controls (Fig. 4A). We also investigated the ability of TFEB to induce the degradation of the polyglutamine (polyQ)–expanded huntingtin protein that is responsible for Huntington's disease using the rat striatal cell model HD43 that carries an inducible transgene for mutant huntingtin (*19*). Immunoblot analyses showed a strong decrease of mutant huntingtin in TFEB-overexpressing cells as compared with those in controls (Fig. 4B). In a parallel experiment, induced HD43 cells were electroporated with a 3xFLAG-TFEB construct. Immunofluorescence analyses showed that the cells that are positive for 3xFLAG-TFEB show little if any huntingtin accumulation (Fig. 4C).

We have discovered a cellular program that regulates lysosomal biogenesis and participates in macromolecule clearance. Lysosomal enhancement as a cellular response to pathogenic accumulation has been observed in neurodegenerative diseases (*20*–*22*). Cathepsin D (*23*, *24*), one of the key enzymes involved in the degradation of neurotoxic proteins, belongs to the CLEAR network and is induced by TFEB overexpression. Also, miR-128 (which we used for TFEB downregulation) is significantly upregulated in the brain of patients with Alzheimer's disease (*25*) and in both prion- and chemical-induced neurodegeneration (*26*, *27*). An appealing perspective would be the use of the CLEAR network as a therapeutic target to enhance cellular response to intracellular pathogenic accumulation in neurodegenerative diseases.

Note added in proof: While this study was in proof, a report was published by Schieweck *et al*. (*28*) in which was shown a lysosomal localization for NCU-G1, the mouse ortholog of Clorf85.

References and Notes

1. P. Saftig, *Medical Intelligence Unit: Lysosomes* (Springer, New York, 2003).
2. J. Reimand, M. Kull, H. Peterson, J. Hansen, J. Vilo, *Nucleic Acids Res.* **35**, W193 (2007).
3. T. Lubke, P. Lobel, D. E. Sleat, *Biochim. Biophys. Acta* **1793**, 625 (2008).
4. M. E. Massari, C. Murre, *Mol. Cell. Biol.* **20**, 429 (2000).
5. N. A. Meadows *et al*., *J. Biol. Chem.* **282**, 1891 (2007).
6. E. Steingrimsson, N. G. Copeland, N. A. Jenkins, *Annu. Rev. Genet.* **38**, 365 (2004).
7. V. A. Gennarino *et al*., *Genome Res.* **9**, 481 (2009).
8. Y. Sancak *et al*., *Science* **320**, 1496 (2008).
9. C. Liang *et al*., *Nat. Cell Biol.* **10**, 776 (2008).
10. Y. Shin, J. Klucken, C. Patterson, B. T. Hyman, P. J. McLean, *J. Biol. Chem.* **280**, 23727 (2005).
11. S. Kornfeld, W. S. Sly, in *The Metabolic and Molecular Basis of Inherited Disease*, vol. 2, C. R. Scriver, W. S. Sly, A. L. Beaudet, D. Valle, Eds. (McGraw-Hill, New York, 2001), pp. 3469–3482.
12. L. E. Karageorgos *et al*., *Exp. Cell Res.* **234**, 85 (1997).
13. A. Helip-Wooley, J. G. Thoene, *Exp. Cell Res.* **292**, 89 (2004).
14. E. F. Neufeld, J. Muenzer, in *The Metabolic and Molecular Basis of Inherited Disease*, C. R. Scriver, W. S. Sly, A. L. Beaudet, D. Valle, Eds. (McGraw-Hill, New York, 2001) pp. 3421–3454.
15. A. Ballabio, V. Gieselmann, *Biochim. Biophys. Acta* **1793**, 684 (2009).
16. J. Muenzer *et al*., *Acta Paediatr. Suppl.* **91**, 98 (2002).
17. K. M. Hemsley, J. J. Hopwood, *Behav. Brain Res.* **158**, 191 (2005).
18. C. Settembre *et al*., *Proc. Natl. Acad. Sci. U.S.A.* **104**, 4506 (2007).
19. S. Sipione *et al*., *Hum. Mol. Genet.* **11**, 1953 (2002).
20. A. M. Cataldo *et al*., *Neuron* **14**, 671 (1995).
21. A. M. Cataldo, J. L. Barnett, C. Pieroni, R. A. Nixon, *J. Neurosci.* **17**, 6142 (1997).
22. J. Bendiske, B. A. Bahr, *J. Neuropathol. Exp. Neurol.* **62**, 451 (2003).
23. U. S. Ladror, S. W. Snyder, G. T. Wang, T. F. Holzman, G. A. Krafft, *J. Biol. Chem.* **269**, 18422 (1994).
24. L. Qiao *et al*., *Mol. Brain* **1**, 17 (2008).
25. W. J. Lukiw, *Neuroreport* **18**, 297 (2007).
26. W. J. Lukiw, A. I. Pogue, *J. Inorg. Biochem.* **101**, 1265 (2007).
27. R. Saba, C. D. Goodman, R. L. Huzarewich, C. Robertson, S. A. Booth, *PLoS One* **3**, e3652 (2008).
28. Schieweck *et al*., *Biochem. J.* 10.1042/BJ20090567 (2009).

29. This paper is dedicated to the memory of Ms. Susanna Agnelli, President of the Italian Telethon Foundation. We thank S. Anand, M. V. Barone, L. Cutillo, M. Morleo, A. Pignata, R. M. Tuzzi, and S. Pepe for technical assistance. We also thank B. Amati, E. Guccione, and P. De Camilli for helpful suggestions and P. Di Fiore, G. Diez-Roux, A. Luini, and C. Missero for comments on the manuscript. This work was supported by the European Union, 7th Framework Program "Euclyd—a European Consortium for Lysosomal Storage Diseases" (health F2/2008 grant agreement 201678) and by the Italian Ministry of Research (PRIN 2006064337). The contributions of the Italian Telethon Foundation and

of the National MPS Society USA are gratefully acknowledged. The authors have no conflicts of interest. Expression microarray data are available at the Gene Expression Omnibus repository under accession number GSE16267. A patent application on the discovery of a gene network regulating lysosomal biogenesis and function has been filed to the European Patent Office (patent application EP 091527788). A.B. and M.S. are inventors on this patent.

Supporting Online Material
www.sciencemag.org/cgi/content/full/1174447/DC1
Materials and Methods
Figs. S1 to S12
Tables S1 to S5
References

2 April 2009; accepted 10 June 2009
Published online 25 June 2009;
10.1126/science.1174447
Include this information when citing this paper.

An ER-Mitochondria Tethering Complex Revealed by a Synthetic Biology Screen

Benoît Kornmann,[1]* Erin Currie,[1]† Sean R. Collins,[2,3]‡ Maya Schuldiner,[4] Jodi Nunnari,[5] Jonathan S. Weissman,[2,3] Peter Walter[1,3]

Communication between organelles is an important feature of all eukaryotic cells. To uncover components involved in mitochondria/endoplasmic reticulum (ER) junctions, we screened for mutants that could be complemented by a synthetic protein designed to artificially tether the two organelles. We identified the Mmm1/Mdm10/Mdm12/Mdm34 complex as a molecular tether between ER and mitochondria. The tethering complex was composed of proteins resident of both ER and mitochondria. With the use of genome-wide mapping of genetic interactions, we showed that the components of the tethering complex were functionally connected to phospholipid biosynthesis and calcium-signaling genes. In mutant cells, phospholipid biosynthesis was impaired. The tethering complex localized to discrete foci, suggesting that discrete sites of close apposition between ER and mitochondria facilitate interorganelle calcium and phospholipid exchange.

Eukaryotic cells evolved segregation of functions into separate organelles. Compartmentalization increases the efficiency of biochemical reactions by creating tailored chemical microenvironments, but also creates a need for communication and routes of metabolite exchange. Membrane lipids, for example, are primarily synthesized in the endoplasmic reticulum (ER) and distributed to other organelles. Many organelles exchange phospholipids with the ER via vesicular transport. In contrast, mitochondria are not connected to vesicular trafficking pathways, and many lipids of the inner and outer mitochondrial membranes (IMM and OMM) cannot be synthesized within mitochondria but are imported by unclear mechanisms. Phospholipids may transfer from the ER to the OMM at spatially restricted sites, which are frequently observed by electron microscopy and have been enriched by cell fractionation (*1*–*3*).

Other work has implicated ER-mitochondrial contact sites in Ca^{++} transport between the ER and mitochondria (*4*–*6*), suggesting a mechanism that may exploit the formation of an encapsulated space at the contact sites, akin to that formed at neuronal or immunological synapses. Such a connection between the ER and the mitochondria might buffer and control cytosolic and mitochondrial Ca^{++} concentrations (*7*). Several proteins have been implicated to participate in ER-mitochondria contacts, including the ER resident Ca^{++} channel IP3 receptor, the mitochondrial voltage-dependent anion channel, the chaperones grp75 and sigma-1R, the sorting protein PACS-2, and the mitofusin Mfn2 (*8*–*11*).

To explore a role for ER-mitochondrial junctions, we sought mutants in the yeast *Saccharomyces cerevisiae*, in which tethering between the two organelles was impaired. We reasoned that, if such contacts are important, defects in proteins that establish these interactions would be detrimental, yet perhaps could be suppressed by artificially tethering ER and mitochondria (Fig. 1A). We designed a synthetic ER-mitochondria tether ("ChiMERA" for construct helping in mitochondria-ER association) (Fig. 1B) consisting of an N-terminal mitochondrial signal sequence and transmembrane domain derived

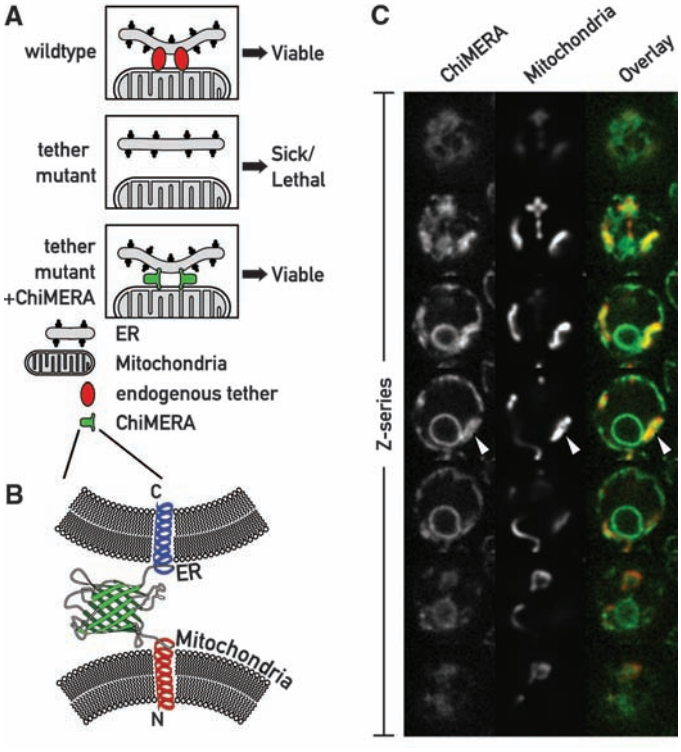

Fig. 1. A synthetic biology screen to uncover mutants of the ER-mitochondria connection. (**A**) Rationale of the screen. (Top) In WT cells a yet unknown endogenous complex tethers the ER to the mitochondria. (Middle) Mutations causing the loss of the endogenous complex are detrimental and cause slow growth or cell death. (Bottom) Artificial ER-mitochondria tethering by ChiMERA can suppress the defects associated with the loss of the endogenous tether. (**B**) Outline of the ChiMERA. A central GFP molecule (green) is flanked by the mitochondria-directed N-terminal Tom70 presequence and transmembrane sequence (red) and the ER-directed C-terminal Ubc6 tail anchor sequence (blue). (**C**) Confocal Z-series across a yeast cell expressing the ChiMERA and a mitochondrial marker (mt-dsRed). ChiMERA displays a characteristic ER staining with additional thicker structures (arrowheads), which colocalize with mitochondria and represent sites of artificial tethering.

[1]Department of Biochemistry and Biophysics, University of California at San Francisco, San Francisco, CA 94158, USA. [2]Department of Cellular and Molecular Pharmacology, University of California at San Francisco, San Francisco, CA 94158, USA. [3]Howard Hughes Medical Institute, University of California at San Francisco, San Francisco, CA 94158, USA. [4]Molecular Genetics, Weizmann Institute of Science, Rehovot, Israel. [5]Molecular and Cellular Biology, University of California at Davis, Davis, CA 95616, USA.

*To whom correspondence should be addressed. E-mail: benoit.kornmann@ucsf.edu
†Present address: Gladstone Institute of Cardiovascular Disease, San Francisco, CA 94158, USA.
‡Present address: Chemical and Systems Biology, Bio-X Program, Stanford University, Stanford, CA 94305, USA.